

## Spectroscopic Identification and Direct Imaging of Interfacial Magnetic Spins

H. Ohldag,<sup>1,2,5</sup> T.J. Regan,<sup>3</sup> J. Stöhr,<sup>1</sup> A. Scholl,<sup>2</sup> F. Nolting,<sup>1,2</sup> J. Lüning,<sup>1</sup> C. Stamm,<sup>1</sup> S. Anders,<sup>2</sup> and R.L. White<sup>4</sup>

<sup>1</sup>Stanford Synchrotron Radiation Laboratory, P.O. Box 20450 Stanford, California 94309

<sup>2</sup>Advanced Light Source, 1 Cyclotron Road, Lawrence Berkeley National Laboratory, Berkeley, California 94720

<sup>3</sup>Department of Applied Physics, Stanford University, Stanford, California 94305

<sup>4</sup>Materials Science and Engineering Department, Stanford University, Stanford, California 94305

<sup>5</sup>Institut für Angewandte Physik, Universität Düsseldorf, Universitätsstrasse 1, 40225 Düsseldorf, Germany

(Received 26 June 2001; published 27 November 2001)

Using x-ray absorption spectromicroscopy we have imaged the uncompensated spins induced at the surface of antiferromagnetic (AFM) NiO(100) by deposition of ferromagnetic (FM) Co. These spins align parallel to the AFM spins in NiO(100) and align the FM spins in Co. The uncompensated interfacial spins arise from an ultrathin CoNiO<sub>x</sub> layer that is formed upon Co deposition through reduction of the NiO surface. The interfacial Ni spins are discussed in terms of the “uncompensated spins” at AFM/FM interfaces long held responsible for coercivity increases and exchange bias. We find a direct correlation between their number and the size of the coercivity.

DOI: 10.1103/PhysRevLett.87.247201

PACS numbers: 75.70.Rf, 75.50.Ee, 78.20.Ls

The determination of the crystallographic, electronic, or magnetic structure of interfaces has remained one of the great challenges in material science owing to the difficulty to detect and isolate the weak interface signature. In particular, many of today's forefront magnetic materials require a better understanding of the spin structure at interfaces [1,2]. Examples are giant magnetoresistance, spin tunnel [3], spintronics [4,5], or exchange biased [6,7] structures. In these structures the magnetic coupling or spin transport across interfaces, involving metals, oxides, or semiconductors, is strongly influenced by the magnetic interface properties. Here we use polarization dependent x-ray spectroscopy and microscopy in electron yield mode for the chemical and magnetic characterization of the Co/NiO(100) interface, including the direct imaging of newly formed interfacial magnetic spins. Interfacial sensitivity is achieved by a unique combination of elemental, chemical, and magnetic specificity and limited probing depth.

We investigated two types of samples. For the x-ray photoemission electron microscopy (XPEEM) measurements [8] a clean NiO(100) surface was obtained by cleaving and in a second step 1.5 nm of cobalt were deposited by molecular beam epitaxy *in situ* using a deposition rate of about 0.4 Å per minute [9]. XPEEM studies utilized the PEEM2 instrument at the Advanced Light Source in Berkeley [10]. The x rays, whose polarization could be changed from linear to right or left circular [8], are incident on the sample at an angle of 30° from the surface. The low-energy secondary electrons from the sample are imaged by an all electrostatic electron microscope with magnification onto a phosphor screen that is read by a charge-coupled device camera. The spatial resolution of PEEM2 is typically 50 nm, sufficient to resolve the antiferromagnetic domain structure of single crystal NiO(100). For the x-ray absorption spectroscopy (XAS) studies we used a structure MgO(100)/NiO(1 nm)/Co(1 nm)/Ru(2 nm) grown by molecular beam epitaxy. Such samples exhibit antiferro-

magnetic NiO domains that are smaller than the resolution of PEEM2 [11], but the ultrathin layers provide high interfacial sensitivity for XAS studies as discussed below. The epitaxial NiO(100) films were grown by electron beam evaporation of elemental nickel in a microwave activated oxygen atmosphere at a typical pressure of  $1 \times 10^{-5}$  torr and a growth rate of 0.3 Å per second [11]. The Co and the Ru layers were also grown *in situ* by electron beam evaporation. The Ru layer prevented oxidation of the Co underneath. The high resolution XAS measurements were carried out on the spherical grating monochromator beam line 10-1 at the Stanford Synchrotron Radiation Laboratory. The measurements employed linearly polarized x rays at normal incidence and total electron yield detection [12].

Figure 1 illustrates the layered structure of our samples and the relative contributions of the layers in the sample to the measured electron yield signal. The characteristic  $(1/e)$  absorption length of the incident x rays ( $\geq 20$  nm) is considerably longer than the secondary electron sampling depth ( $\lambda = 2.5$  nm), and the contribution of the various

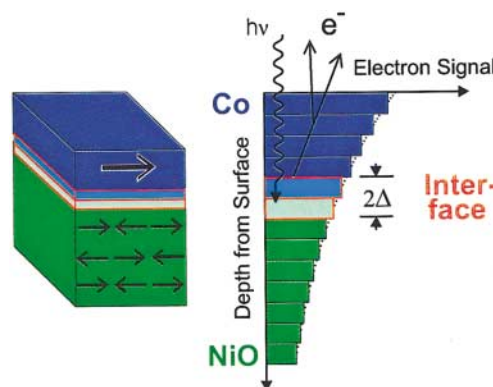


FIG. 1 (color). Layer-by-layer origin of the electron yield signal for a NiO/Co sandwich, assuming equal exponential electron yield decay lengths for Co and NiO.

layers underneath the sample surface is therefore determined by the exponential decay of the electron signal [13]. For a typical value of  $\lambda = 2.5$  nm and a sample of semi-infinite thickness one obtains a 8% contribution of the 1.5 Å thick surface layer. For multilayered samples with finite layer thicknesses the interfacial region contributes a larger fraction [14]. In the presence of a nonmagnetic capping layer like Ru the signals from all underlying magnetic layers are equally attenuated. For the NiO/Co case shown in Fig. 1 the electron signals from the interface and the “bulk” NiO have to traverse the Co film which acts as an attenuator. This attenuation effect limits the study of buried layers or interfaces to a distance of less than about 3 nm from the free surface [8]. The weak interface signal can be isolated from the “bulk” if it exhibits a unique chemical or magnetic signature. For the NiO/Co system this is indeed the case as will be shown below.

Figure 2 illustrates the chemical identification of the interface signal by means of high resolution XAS spectra for the MgO(100)/NiO(1 nm)/Co(1 nm)/Ru(2 nm) sample. The NiO and the Co absorption spectra are detected separately by scanning the photon energy over the respective  $L$  absorption edges of Ni and Co. The fine structure at the

$L_3$  edge in Co and the  $L_2$  edge in Ni, arising from multiplet effects in the oxides [12,15] allows us to further distinguish between metal- and oxidelike samples. Figure 2 directly compares the fine structures of Ni metal and NiO and Co metal and CoO as blue and green curves, respectively. Also shown in red are the XAS spectra for the MgO(100)/NiO(1 nm)/Co(1 nm)/Ru(2 nm) sample, which in both cases are found to be a mixture of the pure metal and oxide spectra. This is quantitatively confirmed by the black curves which are weighted superpositions of the metal and oxide spectra. A detailed analysis [12] shows the formation of a  $2\Delta = 2$  monolayers thick interfacial region consisting of reduced NiO and oxidized Co metal that we shall denote  $\text{CoNiO}_x$ . The spectroscopy data clearly reveal interfacial diffusion effects which are expected to also modify the magnetic structure of the interface. In particular, the reduction of NiO at the interface is expected to create uncompensated spins in the form of a ferrimagnetic or ferromagnetic interface layer.

By tuning the photon energy and selecting circular polarization for Co and linear polarization for Ni we can record the ferromagnetic (FM) domain structure in Co and the antiferromagnetic (AFM) domain structure in NiO [9]. The domain structure is shown for two orientations of the polarized x rays relative to the sample in Figs. 3 and 4. The FM Co domain image was obtained using x-ray magnetic circular dichroism (XMCD) by division of two images taken at the Co  $L_3$  and  $L_2$  (not shown in Fig. 2) edges with circular polarization of the same helicity. The AFM NiO domain image was derived by division of two images taken at the positions of peaks A and B in Fig. 2, using linearly polarized x rays [x-ray magnetic linear

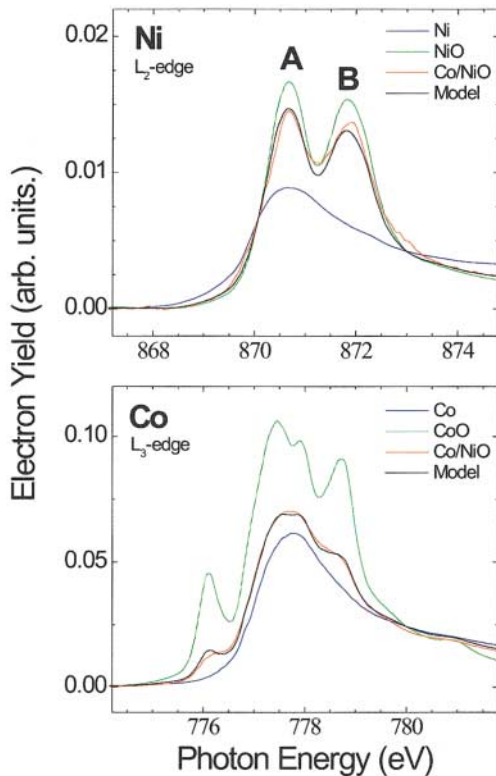


FIG. 2 (color). High resolution x-ray absorption spectra (red) for a MgO(100)/NiO(1 nm)/Co(1 nm)/Ru(2 nm) sample, recorded at the Ni  $L_2$  and Co  $L_3$  edges, in comparison to reference spectra taken for the pure metals (blue) and monoxides (green). The black curve is a weighted superposition of the blue and green spectra.

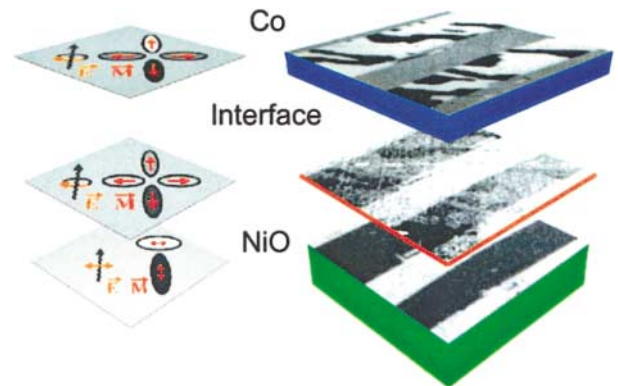


FIG. 3 (color). Circular (XMCD) and linear (XMLD) x-ray dichroism images of a cleaved NiO(100) sample covered by 8 monolayers of Co as grown. The top two rows show FM XMCD images recorded with handed circular polarization at the Co (top) and Ni (middle)  $L$  absorption edges, as discussed in the text. The bottom row shows an AFM XMLD image of NiO recorded with linear polarization. The icons on the left link the contrast with the domain orientations. AFM domain walls are parallel to in-plane [100] directions. The projection of the incoming  $k$  vector onto the sample surface is parallel to [110].

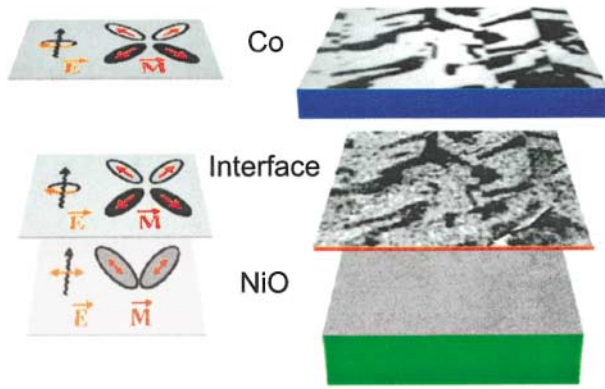


FIG. 4 (color). Images of the same spot as Fig. 3 after in-plane sample rotation by  $45^\circ$ . The in-plane projection of the incoming  $k$  vector is parallel to  $[100]$ . Note that the AFM contrast vanishes in this geometry.

dichroism (XMLD)]. The FM Co spins are found to be aligned collinear to the AFM NiO spins [9], as illustrated by the cartoons on the left side.

We can now utilize the spectroscopic knowledge from Fig. 2 in conjunction with variable x-ray polarization to isolate the magnetic interface signature. In order to look for uncompensated Ni spins at the interface created by chemical reduction of NiO we tune the photon energy to peak A in Fig. 2 which emphasizes a Ni-metal-like component and employ circular polarization. We then record two Ni XMCD images with right and left circular polarization and divide these two images to further increase the FM sensitivity. The resulting images for Co/NiO(100) are shown in the middle of Figs. 3 and 4. The middle image in Fig. 3 appears to be a superposition of the FM Co and AFM NiO image. It clearly shows the characteristic FM signature within the broad stripes. The stripes arise mainly from the non-negligible bulk NiO AFM signal since their black and white contrast is the same as in NiO. While the use of left and right circular polarization emphasizes the FM Ni signal, we still observe a weak linear dichroism effect from the strong NiO signal, caused by the in-plane component of the circularly polarized x rays. However, by rotating the sample to the geometry in Fig. 4 the linear dichroism effect is eliminated and we clearly see the signature of the interfacial Ni spins, alone. The relevant image, shown in the middle, is a one-to-one copy of the Co domain structure. This domain structure is not observed before deposition of the Co layer, and we can conclude from the spectroscopic and microscopic knowledge that the uncompensated spins are created and aligned by the Co deposition. A study of the contrast as a function of excitation energy across the Ni  $L_2$  edge shows that the contrast increases by going from peak B to peak A, as expected from the larger overlap of peak A with the Ni metal peak position (Fig. 2) [16]. Figures 3 and 4 convincingly illustrate the coupling, domain by domain, of the Ni interface layer to both NiO and Co.

The origin of the interfacial spins by a chemical reaction process is corroborated by their increasing number

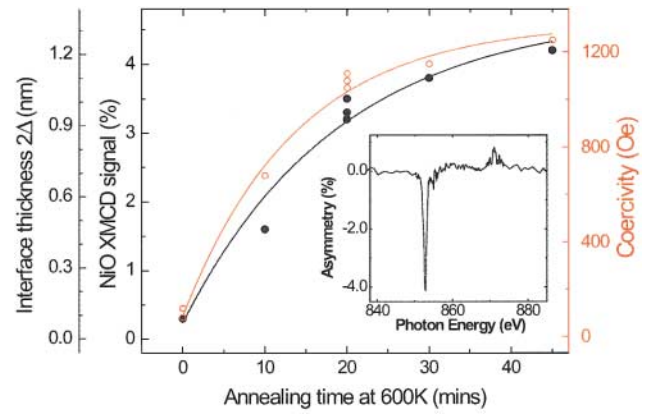


FIG. 5 (color). Dependence of the interfacial spin moment, magnetic interface thickness (black) and coercivity (red) on annealing time at 600 K. The inset shows the XMCD difference spectrum obtained from two ferromagnetic interface domains with opposite magnetization. The black symbols represent the maximum asymmetry in the spectra ( $L_3$  peak at 853 eV) for the initial as-deposited state and after total annealing times of 10, 20, 30, and 45 min. The red symbols are the coercivities of the same films. The fits were obtained using an exponential function  $A - B \exp(-\gamma T)$ .

with temperature. Figure 5 shows the dependence of the XMCD asymmetry, magnetic interface thickness, and coercivity on annealing time to a temperature of 600 K, well above the Néel temperature, as is typically used to introduce a bias by field cooling [6,7]. The XMCD asymmetry is defined as the  $L_3$  peak (853 eV) intensity in the XMCD difference spectrum, shown in the inset, which is a direct measure of the Ni spin moment [17]. The interfacial moment or thickness increase saturates with time, as shown by the exponential fit to the data. This indicates that the chemical process takes place right at the interface, where the oxygen concentration gradient is large in the beginning and decreases with time due to diffusion of oxygen into the Co. The fit indicates a maximum XMCD asymmetry of about 5% or about  $2\Delta = 8$  monolayers ( $\approx 1.5$  nm) of  $\text{CoNiO}_x$ , if we assume a Ni spin moment of  $0.6\mu_B$ , as in the metal. The coercivity increase of the sample as measured by magneto-optical Kerr effect follows the number of uncompensated spins and saturates at about 1350 Oe.

We also investigated the possible formation of antiferromagnetic ordered CoO by oxidation of Co metal at the interface. CoO is an antiferromagnet, whose Néel temperature in a sandwich structure would be above room temperature [18], and it should therefore exhibit a pronounced XMLD effect. Such an effect, with opposite polarization dependence of the 776.1 and 778.7 eV multiplet peaks in Fig. 2, is indeed observed for thin CoO films grown on NiO(100). For Co/NiO(100) samples, however, we were unable to detect any CoO XMLD effect. This leads us to conclude that the oxidation/reduction reaction at the interface creates a mixed magnetically ordered  $\text{CoNiO}_x$  region with neither a pure Ni metal nor pure CoO component.

Our results reveal a different interface structure than assumed in all previous models of AFM/FM interfaces. First, they show the existence of a chemically produced interfacial layer in contrast to the previous assumption of abrupt AFM/FM interfaces. This interface layer naturally gives rise to “uncompensated spins” which have long been associated with coercivity increases and exchange bias in AFM/FM structures [6,7]. In previous models the existence of uncompensated spins was attributed to statistical arguments associated with the termination of bulk antiferromagnetic domains [19], spin-flop canting of antiferromagnetic spins [20], and various defect-based explanations [21,22]. Our measurements show that the observed interfacial spins are responsible for the increased coercivity and coupling strength of Co on NiO(001). Heat treatment increases both the thickness of the interfacial layer and the coupling strength, suggesting that the chemical processes at the AFM/FM interface are essential to establish strong exchange coupling. The fact that the exchange bias field for the samples investigated by us is negligibly small shows that the bias cannot be caused by all interfacial spins, but rather must be due to a small fraction of these spins, probably located at defect sites or domain boundaries. Nevertheless, our results clearly show that a proper description of magnetic coupling at NiO/Co interfaces has to contain the magnetic properties of the identified interfacial layer.

The work was carried out at the Advanced Light Source and the Stanford Synchrotron Radiation Laboratory and is supported by the Director, Office of Basic Energy Sciences of the U.S. Department of Energy. H. O. thanks Professor F. U. Hillebrecht and Professor E. Kisker for their encouragement and support.

---

[1] J. B. Kortright *et al.*, J. Magn. Magn. Mater. **207**, 7 (1999).

- [2] P. Grünberg, Phys. Today **54**, No. 5, 31 (2001).  
 [3] G. A. Prinz, Science **282**, 1660 (1998).  
 [4] R. Fiederling *et al.*, Nature (London) **402**, 787 (1999).  
 [5] Y. Ohno *et al.*, Nature (London) **402**, 790 (1999).  
 [6] J. Nogués, J. Magn. Magn. Mater. **192**, 203 (1999).  
 [7] A. E. Berkowitz and K. Takano, J. Magn. Magn. Mater. **200**, 552 (1999).  
 [8] J. Stöhr *et al.*, Surf. Rev. Lett. **5**, 1297 (1998).  
 [9] H. Ohldag *et al.*, Phys. Rev. Lett. **86**, 2878 (2001).  
 [10] S. Anders *et al.*, Rev. Sci. Instrum. **70**, 3973 (1999).  
 [11] J. Stöhr *et al.*, Phys. Rev. Lett. **83**, 1862 (1999).  
 [12] T. J. Regan, Phys. Rev. B **64**, 214422 (2001).  
 [13] R. Nakajima, J. Stöhr, and I. Idzerda, Phys. Rev. B **59**, 6421 (1999).  
 [14] For interfacial layers of thickness  $\Delta$  on both sides of the Co/NiO interface, as shown in Fig. 1, we obtain an interfacial contribution to the total Co signal of  $F_{Co}^{int} = [e^{-(t-\Delta)/\lambda} - e^{-t/\lambda}]/[1 - e^{-t/\lambda}]$ , where  $t$  is the Co metal thickness. With the values  $t = 1.6$  nm (1.0 nm) for our samples and assuming  $\Delta = 0.2$  nm and  $\lambda = 2.5$  nm we obtain  $F_{Co}^{int} = 9\%$  (17%). For the interfacial layer of thickness  $\Delta$  in NiO we obtain an interface contribution to the total Ni signal of  $F_{NiO}^{int} = [1 - e^{-\Delta/\lambda}]/[1 - e^{-t/\lambda}]$ . With  $t = \infty$  (1.0 nm) for the single crystal and epitaxial sample, we obtain  $F_{NiO}^{int} = 8\%$  (23%), assuming  $\Delta = 0.2$  nm and  $\lambda = 2.5$  nm.  
 [15] F. M. F. de Groot, J. Electron Spectrosc. Relat. Phenom. **67**, 529 (1994).  
 [16] We can exclude that the weak domain structure is caused by a residual Co signal, since the known Co dichroism at the Ni  $L$ -edge position [Srivastava *et al.*, J. Appl. Phys. **83**, 7025 (1998)] is too weak to account for the observed effect.  
 [17] H. Ohldag *et al.*, Appl. Phys. Lett. **76**, 2928 (2000).  
 [18] M. Carey and A. Berkowitz, Appl. Phys. Lett. **60**, 3060 (1993).  
 [19] K. Takano *et al.*, Phys. Rev. Lett. **79**, 1130 (1997).  
 [20] N. C. Koon, Phys. Rev. Lett. **78**, 4865 (1997).  
 [21] T. C. Schulthess and W. H. Butler, Phys. Rev. Lett. **81**, 4516 (1998).  
 [22] P. Miltényi *et al.*, Phys. Rev. Lett. **84**, 4224 (2000).